Proceedings 10th NUMGE 2023
10th European Conference on Numerical Methods in Geotechnical Engineering
Zdravkovic L, Kontoe S, Taborda DMG, Tsiampousi A (eds)

https://doi.org/10.53243/NUMGE2023-304

Modelling of unstable fingered flow in unsaturated soil with Gaussian random fields

E.J. Ricketts[1], P. Cleall[1], A.D. Jefferson[1], P. Kerfriden[2], P. Lyons[3]
[1]*Schoool of Engineering, Cardiff University*
[2]*Centre de Matériaux, Mines Paris – PSL University*
[3]*LUSAS*

ABSTRACT: Hydrological processes in soils, such as fingering and preferential flow, are strongly related to the heterogenous nature of the medium. Such processes can result in accelerated transport of solutes, whilst also causing localised erosion. Neglecting the distinct variation in material properties in numerical simulations can result in an unrealistically uniform wetting front. Here, we represent the variability of the soil mass by random fields, generated through the solution of Whittle-Matérn priors. By solving a stochastic PDE, we avoid the need for large covariance matrices often present in random field generation. As the generated field is an arbitrary representation of correlated space, it can be assigned to represent any spatially varying property. Similarly, it is possible to generate multiple fields for representing spatially varying parameters whose correlation structures differ. Here, we choose the saturated hydraulic conductivity and van Genuchten parameters as they directly affect the hydraulic response of moisture transfer. In doing so, we find that there is accelerated transport in more conductive areas and illustrate this with an example for a hydrophobic soil.

Keywords: Fingered flow, hydrophobicity, stochastics, finite element methods, unsaturated soils

1 INTRODUCTION

Heterogeneity is known to be a cause of nonuniform flow in unsaturated and hydrophobic soils and can lead to fingered flow patterns (Ritsema et al., 1998; Sheng et al., 2014; Sililo and Tellam, 2000). Preferential flow paths form in the soil mass and can transport water at an accelerated rate, resulting in increased rates of solute transport (Gjettermann et al., 1997; Morris and Mooney, 2004; Perkins et al., 2011; Reichenberger et al., 2002), as well as localised erosion. The challenge lies in representing spatial variability in a physically meaningful way without the need for these accelerated flow pathways having an explicit representation in terms of the micro-structure of the porous medium. To be consistent with the soil body structure, the distribution of properties must be correlated with intrinsic length scales, not just a completely random distribution (Lloret-Cabot et al., 2014).

Random fields are a frequently adopted choice when including spatial variability in soil (Arregui-Mena et al., 2016), having been introduced in the seminal work of Vanmarcke (1977). Much of the current literature surrounds random field applications in slope stability (Jiang et al., 2014; Liu and Leung, 2018). More recently, Cueto-Felgueroso et al., (2020) applied intrinsic permeability fields to study the relationship between fingering instabilities and heterogeneity, quantifying the influence of heterogeneity on the resulting infiltration pattern. It was found that heterogeneity amplified the effects of preferential flow, in particular at low infiltration rates as larger infiltration rates tended to smear the developing fingers.

Similar fingered flow patterns also arise when hydrophobicity is present in the soil mass. The presence of water repellency creates highly conductive networks between pores, also known as preferential pathways. Early efforts to model these systems were made by Nieber (1996). The model was based on the well-known Richard's equation and was able to simulate the growth and persistence of a single finger through gravity driven flow. The simulations matched well with experimental observations, highlighting that once a finger begins to form, water will continue to move preferentially through the developed pathway. Further development of the model was conducted in the following years, being applied to solute transport and simulating multiple finger growth due to an advancing wetting front (Nguyen et al., 1999; Nieber et al., 2000). Later, the Richard's equation, upon which the model was formulated, was found to be unconditionally stable (Egorov et al., 2003). To account for this, Nieber et al., (2003) inferred the dynamic response through the mass balance equation. Water repellency was introduced by modifying the saturation-pressure relationship, and it was seen that only a small amount of hydrophobicity was sufficient to

cause unstable flow. It was also concluded that hysteresis was a driving factor in the persistence of the developed fingers.

Similar behaviour was seen through modification of the Soil Water Atmosphere Plant (SWAP) model (Ritsema et al., 2005). The model was applied to an extensive field tracer experiment, showing early arrival times of the bromide tracer due to the influence of water repellent driven flow. The computed and measured bromide concentrations and recovery rates matched well, showing that travel times were significantly reduced, a response that would not be captured if uniform flow was considered. The model was also further developed to analyse the effects of preferential flow on crop growth and solute leaching (Kramers et al., 2005). It was concluded that the physical characteristics of the soil alone did not lead to preferential flow, and neglecting this distinct response prevented the model from being representative of experimental observations.

In this paper we apply an approach presented in a detailed study on modelling infiltration in soils by Ricketts et al. (2023). We generate Gaussian random fields through the solution of a stochastic PDE derived from the Whittle-Matérn autocorrelation function (Roininen et al., 2014). This generation method is computationally efficient and is consistent with the finite element framework employed to solve the wider moisture transport problem. Once generated, the fields are used to represent material properties of the domain, namely the saturated conductivity and van Genuchten parameters. The model is then applied to simulate a layered hydrophobic soil, illustrating the flow characteristics that can be produced.

Section 2 details the theory and numerical discretisation of moisture transport and Gaussian random field generation; Section 3 describes certain numerical details of the field implementation; Section 4 presents an illustrative example of the model's capabilities in representing preferential flow; and Section 5 details the main conclusions of the study and scope for future work.

2 THEORY AND NUMERICAL DISCRETISATION

2.1 Moisture transport

The theoretical model for moisture transport is based on the approach of Cleall et al. (2007), where the soil is assumed to be composed of liquid water and solid mass phases. The influence of the gaseous phase is neglected, such that the volumetric water content θ is solely dependent on the liquid phase. The formulation considers the liquid pressure u_l as a primary variable. The volumetric water content is represented by a mass balance equation depending on degree of saturation and porosity, such that

$$\frac{\partial(\rho_l n S_l)}{\partial t} + \rho_l \boldsymbol{\nabla} \cdot \boldsymbol{v_l} = 0 \tag{1}$$

where ρ_l is the liquid density, n the porosity, S_l the degree of saturation of pore water, and $\boldsymbol{v_l}$ the liquid velocity.

Gradients of total head drive the flow and this is accounted for using Darcy's Law (Darcy, 1856; Hosseinejad et al., 2019; Nielsen et al., 1986; Rosso et al., 2006). For flow in unsaturated soils, this can be expressed as

$$\boldsymbol{v_l} = -\frac{k_l}{\mu_l}\left[\nabla\left(\frac{u_l}{\gamma_l}\right) + \nabla z\right] = -K_l\left[\nabla\left(\frac{u_l}{\gamma_l}\right) + \nabla z\right] \tag{2}$$

where k_l is the effective permeability, μ_l the pore liquid viscosity, γ_l the unit weight of liquid, z the elevation and K_l the unsaturated hydraulic conductivity.

Turbulent effects in the liquid phase may be neglected due to the assumption of flow being slow within the media. Here, the unsaturated hydraulic conductivity is assumed to depend on the degree of liquid saturation and the void ratio. The governing equation for the flow of water can now be formulated by combining the mass conservation equation with Darcy's Law, such that

$$C_{ll}\frac{\partial u_l}{\partial l} - \nabla[K_{ll}\nabla u_l] = J_l \tag{3}$$

where

$$C_{ll} = -n\rho_l\frac{\partial S_l}{\partial s}, \quad K_{ll} = \frac{\rho_l K_l}{\gamma_l}, \quad J_l = \rho_l \nabla(K_l \nabla z). \tag{4}$$

Equation (3) is solved using the Finite Element Method, where the associated discretised equations are derived in the standard way using the Gauss-Green divergence theorem. This results in the following set of equations

$$\begin{aligned}&\int_{\Omega^e} K_{ll}\,\nabla\mathbf{N}^T\nabla\mathbf{N}\,d\Omega\boldsymbol{u_l} + \int_{\Omega^e} C_{ll}\,\mathbf{N}^T\mathbf{N}\,d\Omega^e\frac{\partial\mathbf{u}_l}{\partial t} + \\ &\int_{\Omega^e} K_l\,\rho_l\nabla\mathbf{N}^T\nabla z\,d\Omega^e - \int_{\Gamma^e}\mathbf{N}^T[\rho_l\hat{\mathbf{v}}_l]\,d\Gamma^e = 0\end{aligned} \tag{5}$$

in terms of the array of nodal liquid pressures ($\mathbf{u}_l$), where $\mathbf{N}$ are the shape functions, $\hat{\mathbf{v}}_l$ is the approximate liquid velocity normal to the boundary and e denotes a given element in the discretised domain.

The global matrices are

$$\mathbf{C}_{ll}\frac{\partial\mathbf{u}_l}{\partial t} + \mathbf{K}_{ll}\mathbf{u}_l = \mathbf{F}_l \tag{6}$$

where

$$\begin{aligned}\mathbf{C}_{ll} &= \sum_{e=1}^{m}\int_{\Omega^e} C_{ll}\,\mathbf{N}^T\mathbf{N}\,d\Omega^e,\\ \mathbf{K}_{ll} &= \sum_{e=1}^{m}\int_{\Omega^e} K_{ll}\,\nabla\mathbf{N}^T\nabla\mathbf{N}\,d\Omega^e,\\ \mathbf{F}_l &= \sum_{e=1}^{m}\int_{\Omega^e} K_l\rho_l\nabla\mathbf{N}^T\nabla z\,d\Omega^e - \sum_{e=1}^{m}\int_{\Gamma^e}\mathbf{N}^T[\rho_l\hat{\mathbf{v}}_l]\,d\Gamma^e\end{aligned} \tag{7}$$

and m is the total number of elements in Ω.

An implicit Euler backward difference scheme is employed for time discretisation (Zienkiewicz et al., 2013), such that

$$\mathbf{K}_{ll}\mathbf{u}_l^{t+1} + \frac{1}{\Delta t}\mathbf{C}_{ll}\left(\mathbf{u}_l^{t+1} - \mathbf{u}_l^{t}\right) = \mathbf{F}_l \tag{8}$$

The standard Newton-Raphson procedure is applied (Chitez and Jefferson, 2015), based on a first-order Taylor series expansion of the mass balance error. As such, the primary variable is updated incrementally as

$$\delta\mathbf{u}_l{}_{k+1}^{t+1} = \left[\frac{\partial \boldsymbol{\Psi}}{\partial \boldsymbol{u}_l{}_k^{t+1}}\right](-\boldsymbol{\Psi}) \tag{9}$$

where $\boldsymbol{\Psi}$ is the approximate error given by

$$\boldsymbol{\Psi} = \Delta t\mathbf{K}_{ll}\mathbf{u}_l^{t+1} + \mathbf{C}_{ll}\left(\mathbf{u}_l^{t+1} - \mathbf{u}_l^{t}\right) - \Delta t\mathbf{F}_l. \tag{10}$$

2.2 Gaussian random fields

The generation of Gaussian random fields is based on the approach of Roininen et al., (2014). The field is assumed to be stationary, and as such, the resulting correlated field can be represented by the Matérn autocorrelation function

$$\mathrm{ACF}_{\mathbf{X}}(\mathbf{x}) = \frac{2^{1-\nu}}{\Gamma(\nu)}\left(\frac{|\mathbf{x}|}{l}\right)^{\nu} K_{\nu}\left(\frac{|\mathbf{x}|}{l}\right) \tag{11}$$

for $\mathbf{x} \in \mathbb{R}^d$, where $|\mathbf{x}|$ is the Euclidean distance, $\nu > 0$ is the smoothness parameter, Γ is the gamma function, and K_ν is the Bessel function of the second kind of order ν (Rasmussen and Williams, 2005). The parameter $l > 0$ is the length-scale parameter where $\delta = l\sqrt{8\nu}$ is the distance for correlations near 0.1 (Lindgren et al., 2011), and controls the resulting structure of the correlated fields. Supplying a larger l will result in a highly correlated field with reduced local variation, and a smaller l will increase said local variation.

Equation (11) can be approximated by posing the function as a stochastic PDE, the full details of which are given in Roininen et al. (2014), such that

$$(1 - l^2\Delta)^{\frac{(\nu+d/2)}{2}}\mathbf{X} = \sqrt{\alpha l^d}\mathbf{W} \tag{12}$$

where $d = 1,2,3$, $\mathbf{W}$ is white noise on $\mathbb{R}^d$, and α is a constant defined as

$$\alpha := \sigma^2\frac{2^d\pi^{d/2}\Gamma(\nu+d/2)}{\Gamma(\nu)}. \tag{13}$$

By employing a finite element approximation with the usual Galerkin choice, we are left with a matrix equation which can be solved using standard finite element routines. Similarly, common matrix assembly routines can be utilized due to the resulting matrix components sharing the form of the standard Stiffness and Mass matrix. In solving this equation, we are left with a Gaussian random field that can be used to introduce spatial variability into necessary numerical components such as initial conditions, material properties, or problem geometries.

3 NUMERICAL IMPLEMENTATION

3.1 Field application

The PDE (12) is solved to produce a correlated normalised array with nodal field values relating to the given input mesh. By scaling the generated field based on estimated mean and standard deviation values, we can represent transport parameters in a physically meaningful manner that are necessary for the wider moisture transport problem to be simulated. The choice of parameters are problem dependent and could, for example, include grain size, initial moisture content, or porosity. Here, heterogeneity of the domain is chosen to be dependent on variation in the saturated conductivity and the van Genuchten parameters α_{VG} and n_{VG} where the parameters directly affect the water retention function and unsaturated hydraulic conductivity. The soil water retention function is then calculated as

$$S_l = \left(1 + \left(\alpha_{vg}u_l\right)^{n_{vg}}\right)^{\frac{1-n_{vg}}{n_{vg}}} \tag{12}$$

as in van Genuchten (1980). The imposed variation will lead to banding of the curves, having a distinct relation for a given position in the domain. This choice was made based on the availability of parameter relations and in-situ experimental data.

It is also possible to generate multiple fields whose correlation structures are not related. This is important when representing parameters or conditions whose dynamics should not be dependent on each other. It is also necessary for layered systems as the distinct materials in each layer, whilst having the same physical properties, will have different spatial variations.

3.2 Hydrophobicity

Often, it is only the top layers of a soil body which exhibit water repellent behaviour. This has been observed in contaminated soil, as well as for soils in wildfire affected regions (DeBano, 2000). To account for this within a numerical model, the domain can be divided into layers, where differing statistical properties of material parameters are applied to reflect the presence of hydrophobicity and its effects of flow characteristics. Separate fields are also generated for each layer such that their correlated structures are not related. As many layered soils do not have perfect interfaces between layers, a transition between layers can be applied using a standard sigmoid function that can be tuned appropriately for a smoother or sharper change in material properties with depth.

The differing material properties and their variation will change the infiltration response and allow for more complex interactions, namely accelerated flows in the

more conductive regions, with a build-up of moisture in those less conductive regions. The behaviour may be exaggerated in some layers, appearing more distinct due to the high variability leading to accelerated preferential flow, characteristic to water repellent soils.

4 APPLICATION: HYDROPHOBIC SOIL

Here, an illustrative example is presented which considers a body of soil whose top layer is hydrophobic. This is simulated by having a greater mean value of saturated conductivity and greater variability than the lower layer. The variation and mean value of the van Genuchten parameters also differs between the two layers considered. Example generated fields of saturated conductivity and the van Genuchten parameters are given in Figure 1(a-c), representing a soil mass with dimensions 0.5 x 1 x 0.5 m with a top layer of 0.2 m depth. The numerical domain consists of 15200 uniformly sized 8-noded hexahedral elements.

A surface flux was applied to the top surface of the body for 3.5 hours, resulting in 50 mm of irrigation. The simulation was then continued for a further 24 hours to allow the water to redistribute into the soil body. Figure 2(a-d) show the infiltration profile over time at 700, 2300, 22600, and 99000 seconds respectively, showing the full range of response in the soil mass.

It is clear that the presence of heterogeneity in the media drives unstable flow. When comparing the fields in Figure 1(a-c) with the infiltration profiles in Figure 2(a-d), it is seen that the regions in the field that are less conductive experience a build-up of water which takes a long time to desaturate. The influence of the more conductive top layer is also seen when examining the times between plots in (a-d). The wetting front passes through the top layer quickly, showing characteristics of accelerated preferential flow, and takes much longer to advance having penetrated into the lower layer. The ability of the model to show these type of distinct flow patterns is what distinguishes it from other common approaches, where an assumed homogeneous domain leads to a uniform wetting front.

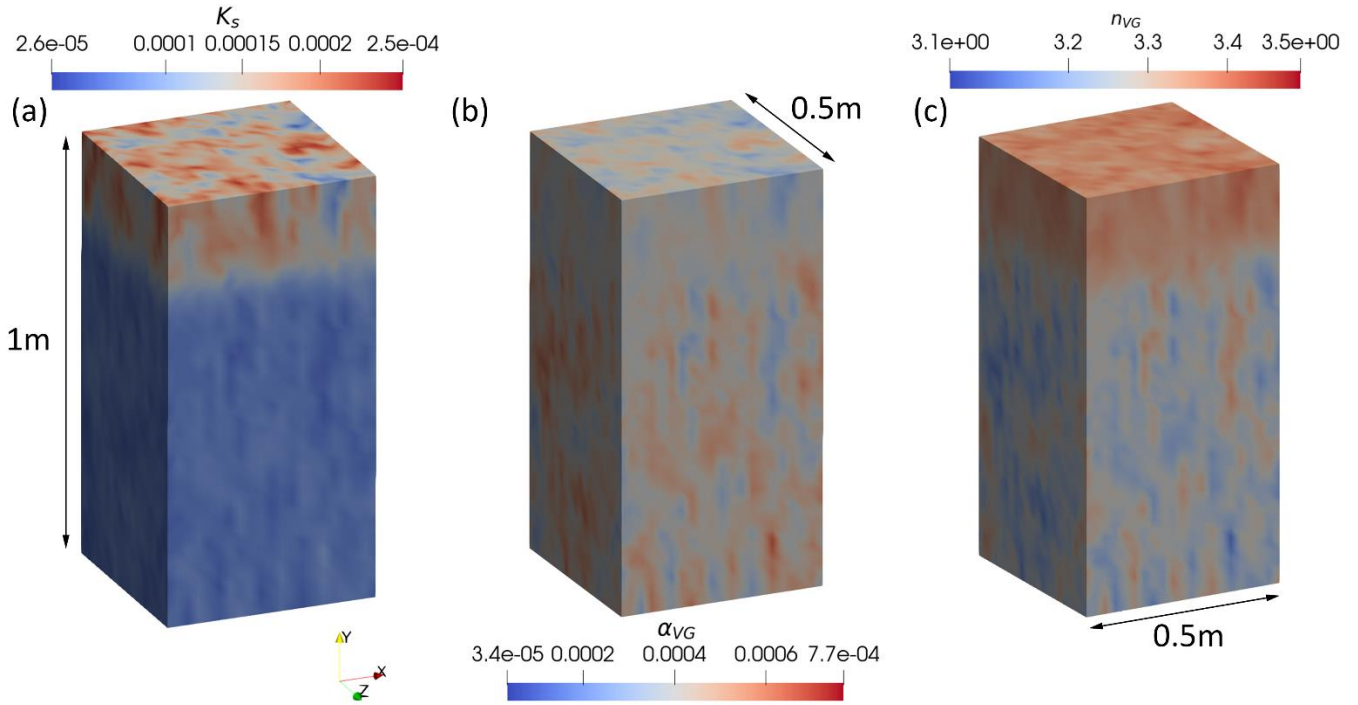

Figure 1: Generated random fields representing (a) saturated hydraulic conductivity and the van Genuchten parameters (b) α_{VG} and (c) n_{VG}

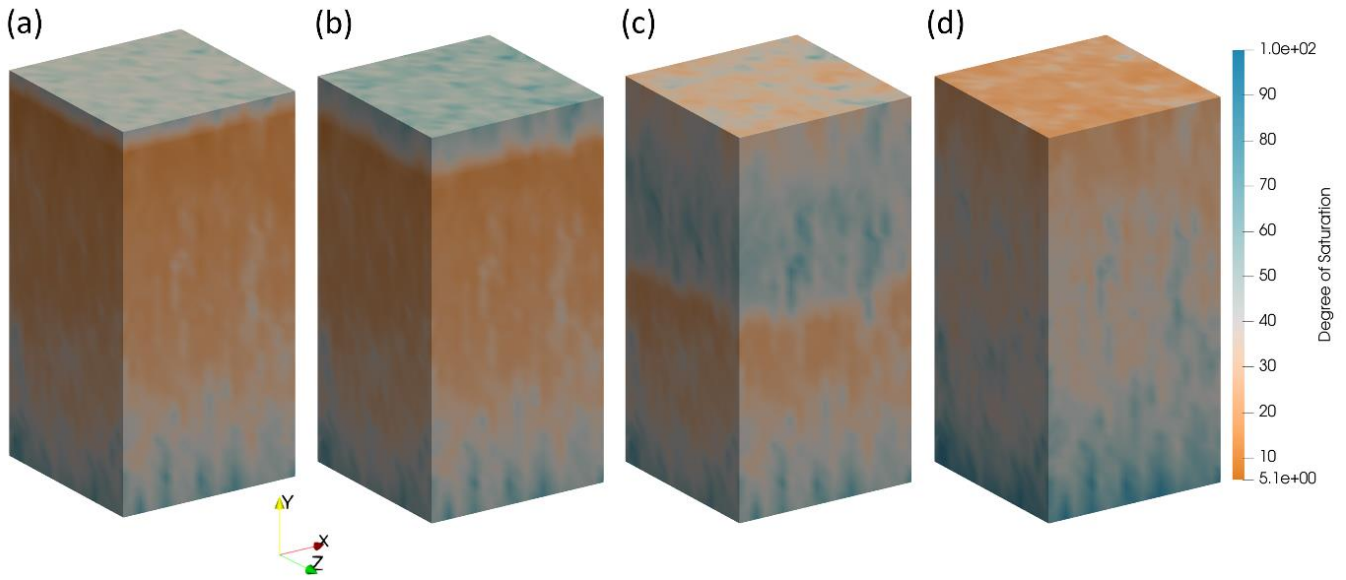

Figure 2: Degree of saturation plots to show surface flux application and the consequent wetting front movement over 24 hours at (a) 700, (b) 2300, (c) 22600, and (d) 99000 seconds

5 CONCLUSION

To enable nonuniform flow in soils to be described with the finite element approach, heterogeneity of the soil mass must be represented in the material properties that govern flow dynamics. Correlated random fields are an obvious choice for this due to their structure being coherent with soil in the field. The approach presented here for random field generation is well suited to the computational structure of FEM codes and does not depend on computationally expensive covariance matrices which can become very large when considering densely meshed 3D problems. The characteristics of flow observed are representative of unstable preferential flow, showing the capabilities of the model in simulating moisture transport in heterogeneous soil.

Similarly, the characteristics of flow in hydrophobic soils can be seen. By accounting for a top layer whose material properties are highly varied compared with the rest of the body, the transfer of moisture is accelerated and is able to pass quickly to deeper regions through distinct preferential flow paths.

Future work is needed to implement constitutive relations to account for varied levels of wettability. The current model treats the soils in all layers as unsaturated, where the unstable flow behaviour is derived from the different levels of spatial variability. Similarly, the application of surface flux should account for the surface variability, where more conductive regions of soil should receive more mass application whilst reducing the total available mass for near-by regions. Combining material specific constitutive relations and more physically meaningful boundary conditions with the current model will enhance the model's ability to represent unstable preferential flow.

6 ACKNOWLEDGEMENTS

The authors would like to acknowledge the School of Engineering at Cardiff University and LUSAS for collectively funding this project.

7 REFERENCES

Arregui-Mena, J.D., Margetts, L., Mummery, P.M., 2016. Practical Application of the Stochastic Finite Element Method. Archives of Computational Methods in Engineering 23, 171–190.

Chitez, A.S., Jefferson, A.D., 2015. Porosity development in a thermo-hygral finite element model for cementitious materials. Cem Concr Res 78, 216–233.

Cleall, P.J., Seetharam, S.C., Thomas, H.R., 2007. Inclusion of Some Aspects of Chemical Behavior of Unsaturated Soil in Thermo/Hydro/Chemical/Mechanical Models. I: Model Development. J Eng Mech 133, 338–347.

Cueto-Felgueroso, L., Suarez-Navarro, M.J., Fu, X., Juanes, R., 2020. Numerical Simulation of Unstable Preferential Flow during Water Infiltration into Heterogeneous Dry Soil. Water (Basel) 12, 909.

Darcy, H., 1856. Les fontaines publiques de la vile de Dijon. Paris, Dalmont.

DeBano, L.F., 2000. The role of fire and soil heating on water repellency in wildland environments: a review. J Hydrol (Amst) 231–232, 195–206.

Egorov, A.G., Dautov, R.Z., Nieber, J.L., Sheshukov, A.Y., 2003. Stability analysis of gravity-driven infiltrating flow. Water Resour Res 39.

Gjettermann, B., Nielsen, K.L., Petersen, C.T., Jensen, H.E., Hansen, S., 1997. Preferential flow in sandy loam soils as affected by irrigation intensity. Soil Technology 11, 139–152.

Hosseinejad, F., Kalateh, F., Mojtahedi, A., 2019. Numerical Investigation of liquefaction in earth dams: A Comparison of Darcy and Non-Darcy flow models. Comput Geotech 116.

Jiang, S.H., Li, D.Q., Zhang, L.M., Zhou, C.B., 2014. Slope reliability analysis considering spatially variable shear strength parameters using a non-intrusive stochastic finite element method. Eng Geol 168, 120–128.

Kramers, G., van Dam, J.C., Ritsema, C.J., Stagnitti, F., Oostindie, K., Dekker, L.W., 2005. A new modelling approach to simulate preferential flow and transport in water repellent porous media: Parameter sensitivity, and effects on crop growth and solute leaching. Soil Research 43, 371.

Lindgren, F., Rue, H., Lindström, J., 2011. An explicit link between Gaussian fields and Gaussian Markov random fields: the stochastic partial differential equation approach, J. R. Statist. Soc. B.

Liu, W.F., Leung, Y.F., 2018. Characterising three-dimensional anisotropic spatial correlation of soil properties through in situ test results. Géotechnique 68, 805–819.

Lloret-Cabot, M., Fenton, G.A., Hicks, M.A., 2014. On the estimation of scale of fluctuation in geostatistics. Georisk: Assessment and Management of Risk for Engineered Systems and Geohazards 8, 129–140.

Morris, C., Mooney, S.J., 2004. A high-resolution system for the quantification of preferential flow in undisturbed soil using observations of tracers. Geoderma 118, 133–143.

Mualem, Y., 1976. A new model for predicting the hydraulic conductivity of unsaturated porous media. Water Resour Res 12, 513–522.

Nguyen, H.V., Nieber, J.L., Ritsema, C.J., Dekker, L.W., Steenhuis, T.S., 1999. Modeling gravity driven unstable flow in a water repellent soil. J Hydrol (Amst) 215, 202–214.

Nieber, J., Sheshukov, A., Egorov, A., Dautov, R., 2003. Non-equilibrium model for gravity-driven fingering in water repellent soils: Formulation and 2D simulations. In: Soil Water Repellency. Elsevier, pp. 245–257.

Nieber, J.L., 1996. Modeling finger development and persistence in initially dry porous media. Geoderma 70, 207–229.

Nieber, J.L., Bauters, T.W.J., Steenhuis, T.S., Parlange, J.-Y., 2000. Numerical simulation of experimental gravity-driven unstable flow in water repellent sand. J Hydrol (Amst) 231–232, 295–307.

Nielsen, D.R., Th. Van Genuchten, M., Biggar, J.W., 1986. Water flow and solute transport processes in the unsaturated zone. Water Resour Res 22, 89S-108S.

Perkins, K.S., Nimmo, J.R., Rose, C.E., Coupe, R.H., 2011. Field tracer investigation of unsaturated zone flow paths and mechanisms in agricultural soils of northwestern Mississippi, USA. J Hydrol (Amst) 396, 1–11.

Rasmussen, C.E., Williams, C.K.I., 2005. Gaussian Processes for Machine Learning. The MIT Press.

Reichenberger, S., Amelung, W., Laabs, V., Pinto, A., Totsche, K.U., Zech, W., 2002. Pesticide displacement along preferential flow pathways in a Brazilian Oxisol. Geoderma 110, 63–86.

Ricketts, E., Cleall, P., Jefferson, A.D., Kerfriden, P., Lyons, P., 2023. Representation of three-dimensional unsaturated flow in heterogeneous soil through tractable Gaussian random fields. (Manuscript submitted for publication).

Ritsema, C.J., Dekker, L.W., Nieber, J.L., Steenhuis, T.S., 1998. Modeling and field evidence of finger formation and finger recurrence in a water repellent sandy soil. Water Resour Res 34, 555–567.

Ritsema, C.J., van Dam, J.C., Dekker, L.W., Oostindie, K., 2005. A new modelling approach to simulate preferential flow and transport in water repellent porous media: Model structure and validation. Soil Research 43, 361.

Roininen, L., Huttunen, J.M.J., Lasanen, S., 2014. Whittle-matérn priors for Bayesian statistical inversion with applications in electrical impedance tomography. Inverse Problems and Imaging 8, 561–586.

Rosso, R., Rulli, M.C., Vannucchi, G., 2006. A physically based model for the hydrologic control on shallow landsliding. Water Resour Res 42.

Sheng, F., Liu, H., Wang, K., Zhang, R., Tang, Z., 2014. Investigation into preferential flow in natural unsaturated soils with field multiple-tracer infiltration experiments and the active region model. J Hydrol (Amst) 508, 137–146.

Sililo, O.T.N., Tellam, J.H., 2000. Fingering in Unsaturated Zone Flow: A Qualitative Review with Laboratory Experiments on Heterogeneous Systems. Ground Water 38, 864–871.

van Genuchten, M.Th., 1980. A Closed-form Equation for Predicting the Hydraulic Conductivity of Unsaturated Soils. Soil Science Society of America Journal 44, 892–898.

Vanmarcke, E.H., 1977. Probabilistic Modeling of Soil Profiles. Journal of the Geotechnical Engineering Division 103, 1227–1246.

Zienkiewicz, O.C., Taylor, R.L., Zhu, J.Z., 2013. The Finite Element Method: its Basis and Fundamentals. Elsevier.